LIFE SCIENCES

Cloning and base editing of GFP transgenic rhesus monkey and off-target analysis

Yu Kang[1,2,3]†, Shaoxing Dai[1,3]†, Yuqiang Zeng[1,3]†, Fang Wang[1,3]†, Pengpeng Yang[1,3], Zhaohui Yang[1,3], Youwei Pu[1,3], Zifan Li[1,3], Xinglong Chen[1,3], Baohong Tian[1,3], Wei Si[1,3], Weizhi Ji[1,2,3]*, Yuyu Niu[1,2,3]*

We report the cloning of a 12-year-old transgenic green fluorescent protein (GFP) monkey by somatic cell nuclear transfer (SCNT) and base editing of the embryos, accompanied with safety evaluation of adenine base editors (ABEs). We first show the ability of ABEmax to silence GFP through A-to-G editing of the GFP sequence in 293T cells. Subsequently, using donor cells from a monkey expressing GFP, we have successfully generated 207 ABEmax-edited (SCNT-ABE) and 87 wild-type (SCNT) embryos for embryo transfer, genotyping, and genome and transcriptome analysis. SCNT-ABE and SCNT embryos are compared for off-target analysis without the interference of genetic variants using a new method named as OA-SCNT. ABEmax does not induce obvious off-target DNA mutations but induces widespread off-target RNA mutations, 35% of which are exonic, in edited monkey embryos. These results provide important references for clinical application of ABE.

INTRODUCTION

Cytosine base editors (CBEs) and adenine base editors (ABEs) can catalyze the conversion of C to T and A to G, respectively, in the target site of a single-guide RNA (sgRNA) (*1*, *2*). Base editors have been demonstrated as potential treatments for genetic diseases by directly correcting their cause, and they have successfully been used for disease treatment in mice and in monkeys in vivo (*3*–*5*). These studies have encouraged further preclinical studies to develop base editors for treating human diseases. However, the concern on off-target effects of the gene editing technology remains. Several studies have shown that CBEs can induce off-target DNA mutations in mouse embryos and in rice (*6*, *7*) and that both CBEs and ABEs can induce off-target RNA mutations in human cells (*8*–*11*). These results have caused big concerns about the efficiency and the safety of using base editors clinically and have demanded comprehensive in vivo analyses of off-target effects of this approach. Before base editors can be used to treat human diseases, we need to prove their safety. Off-targeting analysis of the gene editing approach in nonhuman primates can be a useful reference for the clinical application due to the close genetic relationship of monkeys and humans. However, with genetic variations and technical limitations, it is quite difficult to distinguish off-target mutations from the huge number of single-nucleotide polymorphisms (SNPs) in monkey individuals and to accurately evaluate off-target effects. Here, we developed a method, named as off-target analysis by somatic cell nuclear transfer (OA-SCNT), to evaluate the DNA and RNA off-target mutations induced by the recently reported optimized ABEmax (*12*) in editing monkeys (Fig. 1A). Briefly, we first generated SCNT embryos expressing green fluorescent protein (GFP) using donor cells from a 12-year-old transgenic rhesus monkey expressing GFP and injected ABEmax-encoding mRNA and sgRNA targeting GFP into the one-cell stage SCNT embryos. Edited SCNT and nonedited SCNT blastocysts were then distinguished by GFP expression. For DNA off-target mutation analysis, whole-genome sequencing (WGS) was performed separately on the SCNT-ABE blastocyst and tissues, SCNT blastocyst, and donor cells. Then single-nucleotide variants (SNVs) were called by four algorithms in all samples. Last, off-target mutations were identified in the SCNT-ABE sample, with the SCNT sample as control and the donor cell as the reference. For RNA off-target mutation analysis, we performed RNA sequencing (RNA-seq) on SCNT-ABE and SCNT blastocysts separately, and RNA SNVs were called by GATK. Then RNA off-target mutations were identified in the SCNT-ABE blastocyst, similar to analysis of the DNA off-target mutation.

RESULTS

ABEmax induces A-to-G base conversion in the coding sequence of GFP

First, we tested whether the ABEmax system could mediate the site-specific A·T-to-G·C conversion in the coding sequence of GFP in 293T cells. A specific target site of the GFP gene was selected, and an sgRNA was designed to introduce a point mutation to this site (199 A to G of the antisense strand, Tyr^{66}His) (fig. S1A). This single A-to-G conversion at the target site silenced green fluorescent expression (fig. S1, B and C). On the basis of the on-target analysis by sequencing subcloned polymerase chain reaction (PCR) products, the targeted point mutation [position A_4, counting the protospacer adjacent motif (PAM) sequence as positions 21 to 23] was observed with an efficiency of 40% (8 of 20) and a mutation at the position A_9 that harbored the same A-to-G mutation in a heterozygous manner was also found (5%, 1 of 20) (fig. S1D).

Next, embryos expressing GFP were obtained by SCNT using cells from a 12-year-old transgenic GFP monkey reported previously (fig. S2, A to D) (*13*). We then carried out base editing in SCNT embryos by microinjection of ABEmax-encoding mRNA and sgRNAs to silence the GFP expression (Fig. 1B and fig. S2E). Targeted point mutation (A_4-to-G_4 conversion) was observed in 32 of 40 (80%) SCNT-ABE embryos with mutation frequencies ranging

[1]State Key Laboratory of Primate Biomedical Research, Institute of Primate Translational Medicine, Kunming University of Science and Technology, Kunming, Yunnan 650500, China. [2]Faculty of Life Science and Technology, Kunming University of Science and Technology, Kunming, Yunnan 650500, China. [3]Yunnan Key Laboratory of Primate Biomedical Research, Kunming, Yunnan 650500, China.
*Corresponding author. Email: niuyy@lpbr.cn (Y.N.); wji@lpbr.cn (W.J.)
†These authors contributed equally to this work.

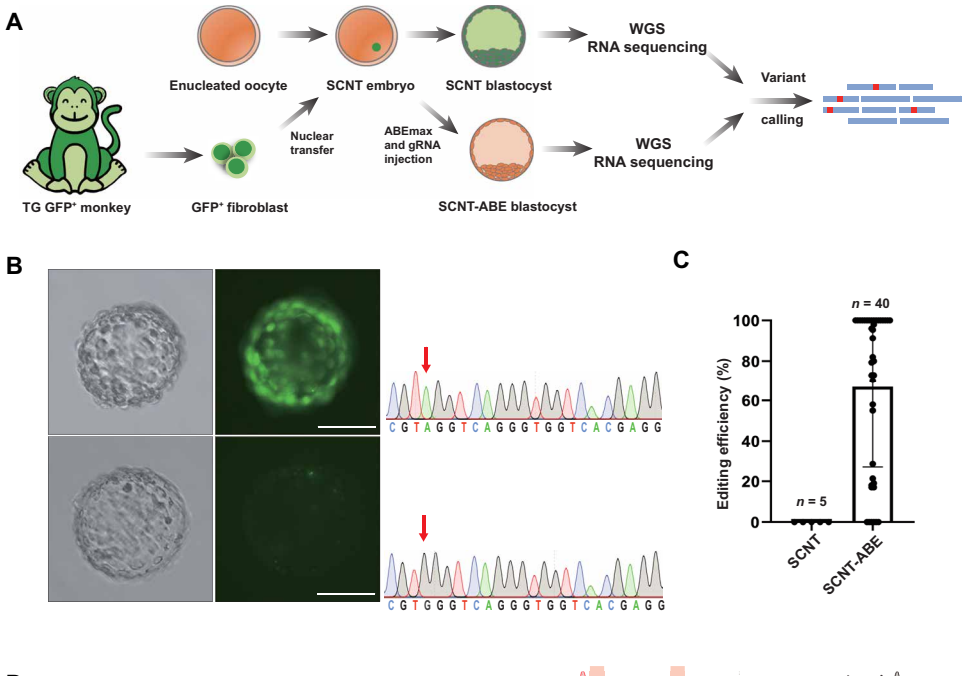

F

Embryo type	No. of total embryos	No. of genotyped embryos	No. of embryos for WGS	No. of embryos for RNA-seq	No. of transferred embryos	No. of surrogate monkey	No. of pregnant monkey	No. of aborted monkey	No. of born monkey	No. of survived offspring
SCNT	87	5	9	5	68	18	3	3	0	0
SCNT-ABE	207	40	8	5	154	31	5	4	1	0

Fig. 1. ABE-mediated GFP knockout in SCNT monkey. (**A**) The scheme of experimental procedures. TG, transgenic. (**B**) Representative images of ABE-mediated GFP silencing in SCNT monkey embryos. Top: SCNT blastocyst generated from transgenic GFP monkey. Bottom: GFP silencing in ABE-editing SCNT blastocyst. Left: Bright field. Right: GFP. Scale bars, 100 μm. (**C**) On-target analysis of ABE editing (the percentage of mutant cells in total blastomere) in monkey SCNT and SCNT-ABE embryos. (**D**) Image of the newborn cloned rhesus monkey generated by SCNT using adult transgenic rhesus monkey fibroblast. (**E**) On-target sequencing of donor cells and tissues of SCNT-ABE monkey. (**F**) Summary of rhesus SCNT embryos used in this study.

from 17 to 100% (Fig. 1C and table S1). The rate for on-target homozygous conversion from A_4 to G_4 was 37.5% (15 of 40), and a bystander mutation of A_9-to-G_9 conversion was also observed in 12.5% (5 of 40) of embryos (fig. S2F and table S1). The edited embryos showed a reduced or silent green fluorescent, consistent with its mutant genotype (Fig. 1B and fig. S2E). Overall, these results suggested that the ABEmax system was highly efficient in the conversion of the A·T base pair to G·C in monkey SCNT embryos.

Generation of SCNT-ABE embryos and monkey

To analyze potential genome-wide off-target effects of ABE, we established a total of 294 embryos, including 87 SCNT embryos and 207 ABEmax-edited SCNT (SCNT-ABE) embryos, from 341 metaphase II (MII) stage oocytes (Fig. 1F). Next, a total of 68 SCNT embryos were transferred into 18 surrogate monkeys, which were transferred with three to four embryos each, to establish SCNT monkeys, whereas 154 SCNT-ABE embryos were transferred into 31 surrogate monkeys to establish SCNT-ABE monkeys. Pregnancy rates of SCNT and SCNT-ABE groups were 16.67 (3 of 18) and 27.78% (5 of 31), respectively. Most fetuses were miscarried in early pregnancy, only two pregnancies in the SCNT-ABE group developed beyond 130 days, and one of them yielded a live birth on day 154 via cesarean section. Unfortunately, the SCNT-ABE monkey died 12 hours later (Fig. 1D, fig. S3A, and movie S1). We observed

amniotic fluid deficiency and placental insufficiency during gestation of this clone monkey fetus, coupled with acute heart rate decrease before cesarean. With autopsy and pathological examination of the cloned monkey, we identified the major pathological changes as internal hemorrhage in the lung, spleen, and kidney (fig. S3, B to D) and partial glass-like degeneration of renal tubular epithelial cells (fig. S3E). On the basis of the above diagnosis, we presumed that the cause of death was multiple organ dysplasia resulting from intrauterine fetal anoxia. The extremely low cloning rate, due to undiscovered epigenetic barriers in postimplantation stage, is still a big problem in the SCNT technique (*14*). SCNT embryos frequently exhibit abnormalities in extraembryonic tissues, leading to birth defect (*15*, *16*). In our research, the pregnancy rate was not substantial different between SCNT and SCNT-ABE groups. At this point, we consider the cause of death of this cloned monkey as the development defect of SCNT embryos rather than ABEmax editing.

To confirm the genetic origin of this cloned monkey, we analyzed SNPs of its mitochondrial DNA (mtDNA) and short tandem repeats (STRs) of its nuclear DNA. We found that all SNPs of the mitochondrially encoded NADH: ubiquinone oxidoreductase core subunit 3 (MT-ND3) gene of the SCNT-ABE monkey were identical to those of its oocyte donor monkey but different from those of the surrogate monkey and donor fibroblasts, consistent with the predominant contribution of donor oocyte mtDNA to the total mtDNA of SCNT embryos (fig. S3F). A total of 14 nuclear loci were used for STR analysis, and the result showed that the nuclear DNA of SCNT-ABE monkey was the same as that of the donor transgenic GFP monkey fibroblasts but different from those of the surrogate monkeys and oocyte donors (fig. S3G).

Since the donor fibroblasts for SCNT were from a 12-year-old transgenic GFP monkey, the SCNT monkey is supposed to express GFP, as shown in the SCNT embryo (fig. S2D). PCR and Sanger sequencing were performed to determine the genotype of SCNT-ABE monkey at the target loci of the sgRNA. Genotyping of five tissues showed that the SCNT-ABE monkey carried the expected A_4-to-G_4 and A_9-to-G_9 mutations with 100% frequency at the target locus (Fig. 1E and fig. S4A). This is identical to the mutation genotype of SCNT embryos described above. Examination under ultraviolet light revealed that the SCNT-ABE monkey did not express GFP (fig. S3A), consistent with its mutant genotype. GFP expression in different organs, both in tissue sections (fig. S4B) and in cultured fibroblast cells, was further examined (fig. S4C). These results demonstrated that the SCNT-ABE monkeys, unlike its transgenic founder monkey, did not express GFP in any examined tissues. In summary, we performed SCNT using adult transgenic rhesus monkey fibroblasts and successfully produced live birth of monkey offspring with A-to-G base editing.

ABEmax does not induce obvious off-target DNA mutation

To explore the potential genome-wide off-target effect of ABEmax, we performed WGS at an average depth of 60× on 11 SCNT and 11 SCNT-ABE samples (see details in Materials and Methods). The donor cell samples were also subjected to WGS and used as the reference. Figure S5A shows the workflow of whole-genome off-target SNV analysis. We called SNVs in SCNT-ABE samples using four software tools, with SCNT samples from the same GFP^+ fibroblast as the control, and obtained on-target editing rate from the WGS data through mapping the reads to the GFP sequences. The on-target editing rate ranged from 72 to 100% in SCNT-ABE samples, whereas no editing was found in any SCNT samples (fig. S6). The SNVs of each sample identified by each of the four software tools are shown in fig. S7. The numbers of SNVs in the SCNT-ABE group showed no difference from those of the control group (mean: 125 versus 84, SD: 107.43 versus 22.99, $P = 0.87$) (left graph in Fig. 2A). We observed that the variation of SNP numbers in the ABE group was much larger than that in the control group, suggesting that some other factors such as cell cycle phase could affect off-target editing outcomes. Cell division occurs rapidly during early embryonic development. Therefore, ABE might only cut a single allele at different cell cycle phases, which led to heterogeneity in ABE-edited embryos. Besides SNV, we also analyzed small indel, copy number variant (CNV), and structural variant (SV) between the two groups. The number of small indel in the SCNT-ABE group was not significantly different from that in the SCNT group (mean: 43 versus 48, SD: 30.80 versus 18.74, $P = 0.19$) (right graph in Fig. 2A). For CNV, both SCNT-ABE and SCNT groups had similar patterns with donor cell samples (fig. S8A). For SV, SCNT-ABE and SCNT groups had comparable numbers of large deletions, duplications, inversions, and translocations (fig. S8B), whereas the number of large insertions in the SCNT-ABE group was higher than that in the control group (fig. S8B).

We classified SNVs into different mutation types and compared each mutation type between SCNT-ABE and SCNT groups. Although the average numbers of A>G/T>C and C>T/G>A SNVs in SCNT-ABE embryos were higher than those in SCNT embryos (Fig. 2B), there was no significant difference for the A>G/T>C ($P = 0.38$) and C>T/G>A ($P = 0.47$) SNVs or any other SNVs (A>C/T>G, A>T/T>A, C>G/G>C, and C>A/G>T) (Fig. 2C). Note that percentages of A>G/T>C and C>T/G>A transition showed some differences between SCNT-ABE and SCNT embryos (Fig. 2D) due to large variation of SNVs in some SCNT-ABE embryos. We further mapped the genomic distribution of A>G and C>T SNVs and found that these SNVs were distributed in different gene regions [untranslated region (UTR), exonic, intronic, downstream, upstream, and intergenic] (Fig. 2, E and F). The number of A>G and C>T SNVs in all regions showed no difference between the two groups (Fig. 2, E and F). We further analyzed the adjacent 3–base pair (bp) sequences of DNA A>G and C>T off-target mutations between the two groups and did not find any specific motif enriched in the SCNT-ABE group compared with the SCNT group (figs. S9 and S10). These data demonstrated that ABE did not generate obvious DNA off-target mutation.

ABEmax induces transcriptome-wide RNA off-target editing

Base editors had been reported to induce transcriptome-wide off-target editing (*8*, *9*), we therefore evaluated these potential effects induced by ABEmax in five SCNT-ABE blastocyst samples through RNA-seq using five SCNT blastocysts as controls and WGS of cell donor as the reference (fig. S5B). For all five SCNT-ABE blastocysts, the editing efficiency of on-target site was higher than 50% (fig. S11A). We found a higher number of off-target RNA edits in SCNT-ABE blastocyst, which was entirely contributed by the A>G RNA edits, when compared with SCNT blastocyst ($P = 0.0317$) (Fig. 3A). The number of the A>G RNA edit in SCNT-ABE blastocysts was significantly higher than that in SCNT blastocyst (mean: 7888 versus 2297, SD: 3738 versus 820, $P = 0.0079$) (Fig. 3A and fig. S11B). Furthermore, the percentage of A>G/T>C transition in the SCNT-ABE group was higher than that in the SCNT group ($P = 0.0079$) (Fig. 3B

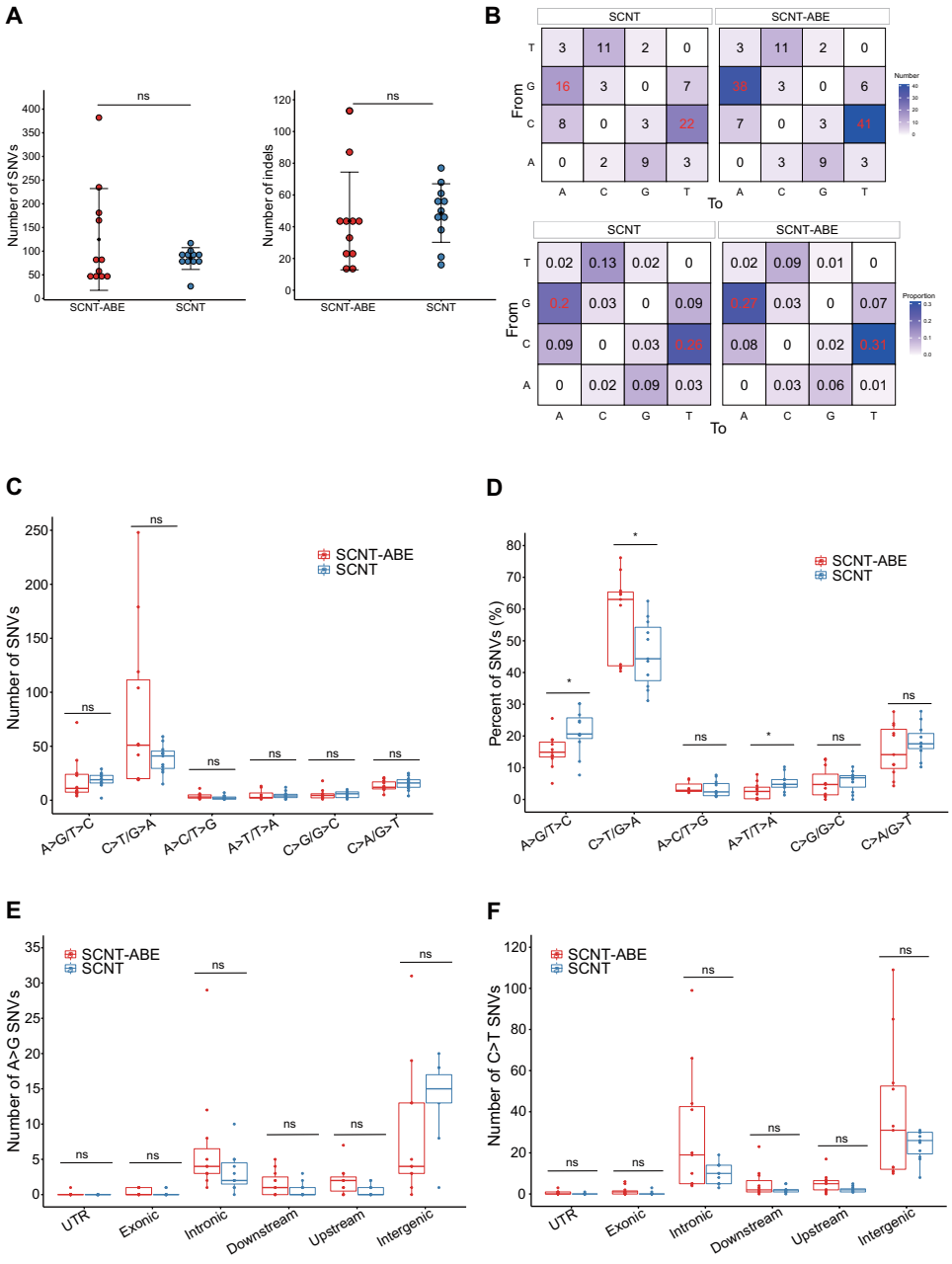

Fig. 2. Comparison of SNVs and indels generated in SCNT-ABE and SCNT groups. (**A**) Dot plot showing numbers of SNVs (left) and small indels (right) between SCNT and SCNT-ABE groups. Both SNVs and small indels in SCNT-ABE group are similar to those of the control group ($P = 0.87$ and $P = 0.19$, respectively). (**B**) Heatmap showing the number (top) and proportion (bottom) of different mutation types between SCNT and SCNT-ABE groups. A gradient of gray and blue indicates low to high number or proportion of SNVs. Each value represents the average value of different mutation types in SCNT or SCNT-ABE groups. (**C**) Comparison of the number of different types of off-target SNVs detected in SCNT and SCNT-ABE samples. (**D**) The proportion of different types of off-target SNVs detected in SCNT and SCNT-ABE samples. (**E** to **F**) Comparison of the number of A>G (E) and C>T (F) off-target SNVs in different genomic regions between SCNT and SCNT-ABE samples. *P* values shown above the horizontal bars were calculated by two-sided Wilcoxon rank sum test. $P < 0.05$ was considered significant in (A) and (C) to (F). *$P < 0.05$. ns, not significant.

and fig. S11C). Because of the very high percentage of A>G/T>C transition in the SCNT-ABE group, percentages of other types of off-target RNA mutations in the SCNT-ABE group were significantly lower than those in the SCNT group (Fig. 3B). We also checked the number of each RNA mutation types within the SCNT-ABE group and the SCNT group. The number of A>G/T>C mutations was higher than that of C>T/G>A mutations in the SCNT-ABE group ($P = 0.0079$), but they were similar in the SCNT group (Fig. 3, C and D, and fig. S11, D and E). The frequencies of the adenine edits that we identified in SCNT-ABE blastocysts ranged from 6 to 100% (mean of 30.28% with 95% confidence interval of 30.07 to 30.50%; Fig. 3E), and these edits were distributed throughout the transcriptome (Fig. 3F and fig. S11, F to I). More than 98% of these edits occurred in the protein-coding genes, and only 1.9% of off-target

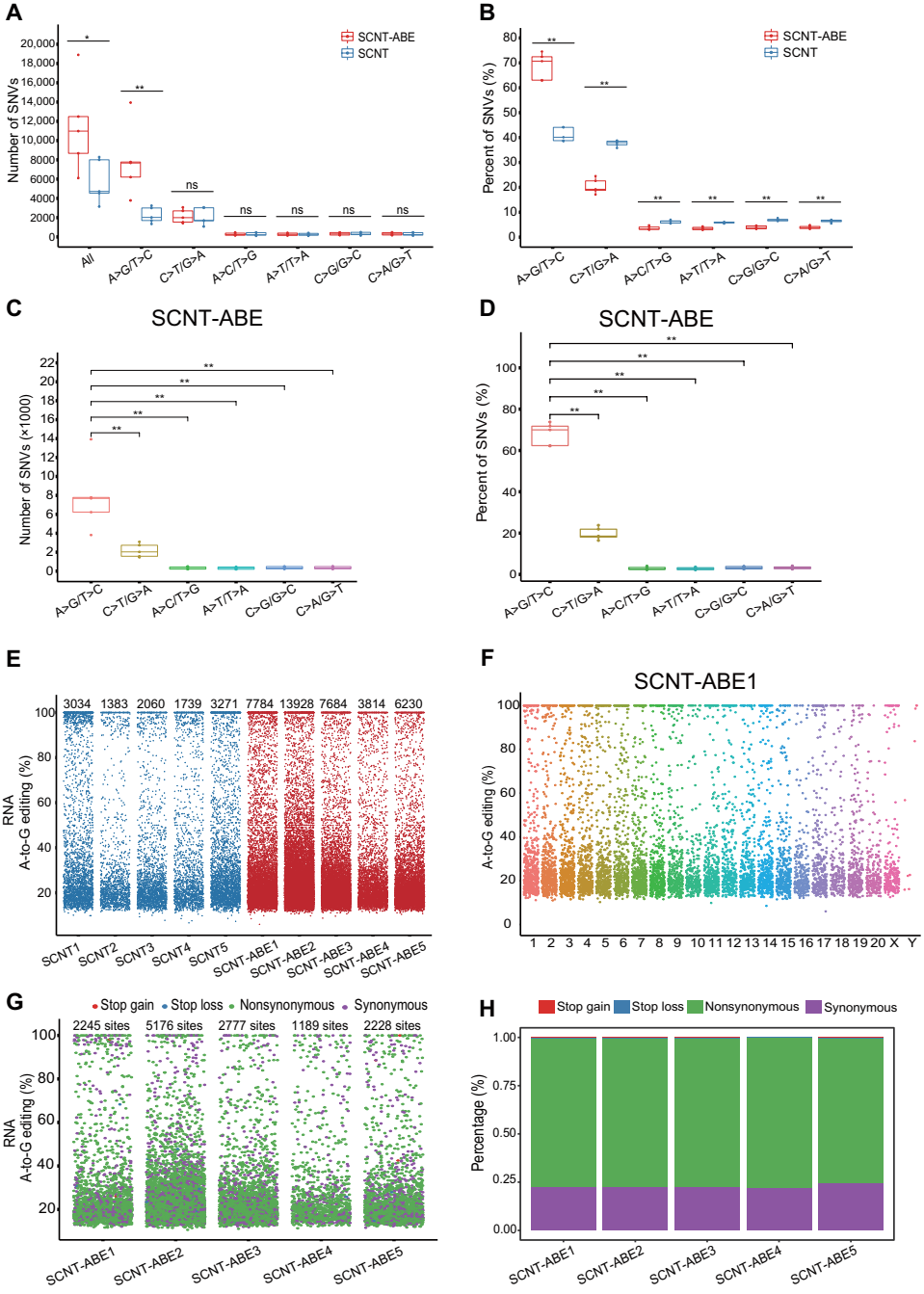

Fig. 3. ABE induces transcriptome-wide off-target A-to-G RNA editing in monkey embryos. (**A**) Comparison of the number of all types and indicated types of off-target RNA mutation detected in SCNT and SCNT-ABE blastocyst. Both numbers of the total and of A>G RNA mutations in SCNT-ABE blastocyst are significantly higher than that in SCNT blastocyst ($P = 0.0317$ and $P = 0.0079$, respectively). (**B**) The proportion of indicated types of off-target RNA mutation detected in SCNT and SCNT-ABE blastocyst. (**C** and **D**) The number (C) and proportion (D) of different types of off-target SNVs detected within SCNT-ABE blastocyst. (**E**) Jitter plots showing efficiencies of A>G RNA editing by ABE derived from RNA-seq experiments. Samples of SCNT1 to SCNT5 and SCNT-ABE1 to SCNT-ABE5 are from SCNT and SCNT-ABE blastocyst, respectively. Top: The number of A>G RNA mutation for each sample. (**F**) Jitter plot showing the distribution of editing rate for each off-target A>G RNA mutation on monkey chromosomes for sample SCNT-ABE1 from (E). Chromosomes are indicated with different colors. (**G**) Jitter plots showing the editing rate of A>G RNA editing occurred in exons for SCNT-ABE blastocyst. Each dot represents the editing rate of one editing site in (E) to (G). The editing rate was calculated as the number of mutated reads divided by the sequencing depth for each site. (**H**) The stacked bar chart showing proportion of different exonic edits from (G). *P* values shown above the horizontal bars were calculated by two-sided Wilcoxon rank sum test. *$P < 0.05$; **$P < 0.01$.

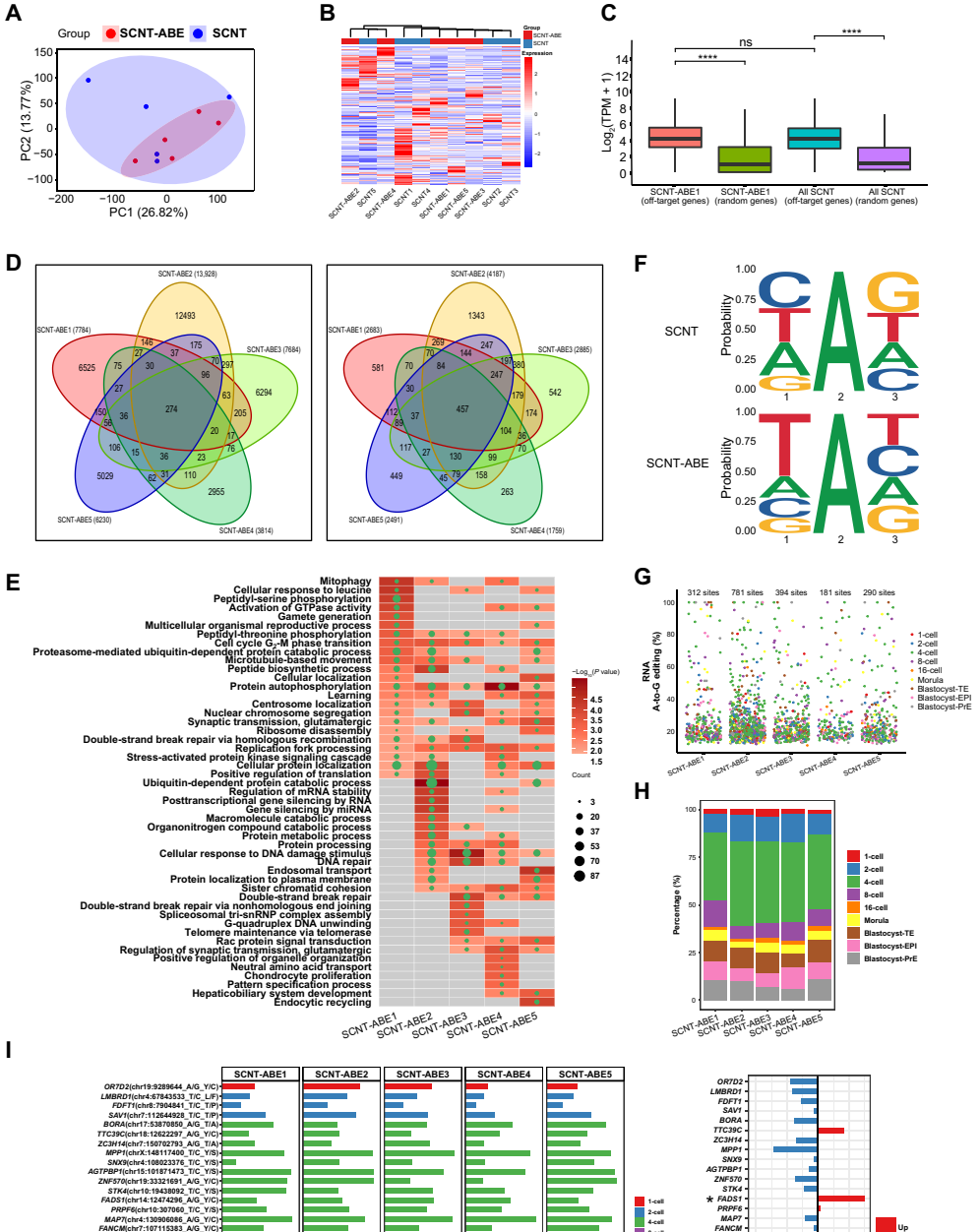

Fig. 4. Characterization of off-target RNA mutations. (**A** and **B**) Principal components (PC) analysis (A) and heatmap (B) showing the clustering of samples from SCNT and SCNT-ABE blastocysts based on the overall gene expression. (**C**) Boxplot showing the expression of genes containing off-target RNA mutations (off-target genes) and random simulated genes (random genes) in SCNT-ABE1 and all SCNT samples. TPM, transcripts per million. (**D**) The Venn diagram showing overlapped editing sites (left) and genes (right) among five SCNT-ABE blastocysts. (**E**) Gene ontology (GO) biological process enriched by the RNA off-target editing genes from (D) in five SCNT-ABE blastocysts. GTPase, guanosine triphosphatase; snRNP, small nuclear ribonucleoprotein. (**F**) Sequence logos derived from A>G RNA mutations in all SCNT (top) and SCNT-ABE (bottom) blastocysts. (**G**) Jitter plots showing the editing rate of A>G exonic edits in the key genes at different stages of embryo development for SCNT-ABE blastocyst. Each dot represents the editing rate of an editing site. TE, trophectoderm; EPI, epiblast; PrE, primitive endoderm. The editing rate was calculated as the number of mutated reads divided by the sequencing depth for each site. (**H**) The stacked bar chart showing proportion of different edits from (G). (**I**) The bar chart showing the editing rate (15 to 100%) of 32 common editing sites in all five SCNT-ABE samples (left) and the expression of the corresponding gene (right). Significantly up- or down-regulated genes are marked with an asterisk before it. FC, fold change. *P* values shown above the horizontal bars were calculated by two-sided Wilcoxon rank sum test. ****$P < 0.0001$.

RNA edits occurred in long intergenic noncoding RNAs (fig. S11, J and K). About 35% edits occurred in the exon region (Fig. 3G), more than 75% of which were nonsynonymous mutations (Fig. 3H).

We explored the relationship between gene editing and gene expression and found that there was no clear distinction in the overall gene expression between SCNT-ABE and SCNT blastocysts (Fig. 4, A and B), implying that ABE editing did not change the overall gene expression significantly. In the SCNT-ABE group, the expression of off-target edited genes was significantly higher than that of the other randomly selected genes (Fig. 4C). This suggested that RNA off-target editing tended to occur in highly expressed genes. However, the high expression of these genes was not due to the gene editing itself, because the expression of these genes between SCNT and SCNT-ABE groups was not significantly different (Fig. 4C). This trend was observed in all SCNT-ABE samples (fig. S12). Rather than changing gene expression, the main effect of ABEmax was to induce off-target RNA mutations that could change protein sequence and its function. Only a small proportion of off-target mutation sites (274) and about a quarter of off-target mutation genes (472) were shared among all five SCNT-ABE samples (Fig. 4D), suggesting that the ABE off-target editing could occur at different genes that were associated with different biological processes (Fig. 4E).

Further analysis of the adjacent 3-bp sequences of RNA A>G/T>C off-target mutations between the two groups revealed that, consistent with previous studies (*8*, *9*), edited adenines were preferentially within a consensus UA (TA) motif in the SCNT-ABE group, which differs from the motifs in SCNT group (Fig. 4F and fig. S13). Last, we assessed the potential effect of RNA A>G/T>C off-target mutations on embryo development and oncogenicity. For each sample, on average, 392 editing sites occurred in exons of key genes in different stages of embryo development (Fig. 4G). On average, 3, 12, 41, 9, 2, 5, 10, 9, and 9% of key genes for 1-, 2-, 4-, 8-, and 16-cell stages; morula; blastocyst trophoderm; blastocyst epiblast; and blastocyst primitive endoderm, respectively, were edited (Fig. 4H). We found that 32 editing sites were common in all five SCNT-ABE samples (Fig. 4I), with the editing rate ranging from 15 to 100%. These edits could cause changes in protein sequences but had little effect on gene expression; only the fatty acid desaturase 1 (FADS1) gene was significantly up-regulated (Fig. 4I) in SCNT-ABE samples. Similarly, RNA A>G/T>C off-target mutations also could affect the oncogenicity (fig. S14). For each sample, on average, 109 editing sites occurred in the exons of oncogenes or tumor suppressor genes (TSGs) (fig. S14A), with a relatively large proportion of editing sites occurred in TSG (fig. S14B). We found eight editing sites common among all five SCNT-ABE samples, which changed protein sequence but had little effect on gene expression (fig. S14C). However, because of resource and technical limitations, it is unpractical to obtain a large number of monkey SCNT embryos to perform proteomic analysis at the moment, and the proteomic changes at the embryo level still need further research.

DISCUSSION

ABEs have successfully been used for disease treatment in nonhuman primates (*3*, *4*). However, a major concern of the genome-editing approach is off-target editing, a comprehensive analysis of off-target effects caused by genome editing is therefore required for its clinical development. Several methods have been developed to detect genome-wide off-target mutations (*17*–*20*), but these approaches are not applicable to detect SNVs in vivo, especially in primates. Here, we report the development of the OA-SCNT method to examine off-target effects of base editors in different primate individuals. We demonstrate that ABEmax does not induce obvious off-target DNA mutation but cause substantial off-target RNA mutations in monkey embryos. These results are consistent with previous studies in the rice and the mouse (*6*–*9*). We identify many off-target RNA mutations that are nonsynonymous mutations with potential impacts on embryo development and oncogenicity. These findings have important implications for the application of base editors in both research and clinical settings. Although edited RNAs only exist for a short period of time, the influence of RNA mutations should be minimized for therapeutic applications in humans.

Consideration of technical limitations, the OA-SCNT method is more suitable for primates than the genome-wide off-target analysis by two-cell embryo injection (GOTI) method (*6*). Since all embryos in both SCNT and SCNT-ABE groups originate from the donor cells, OA-SCNT method avoids interference of genetic variants and is optimal to identify off-target SNVs. Therefore, besides the reference genome Mmul_8.0.1, the genome of the donor cell is also used as a reference in the OA-SCNT method. This helps in identifying the SNVs more precisely in edited samples because of differences between the genome of the experimental sample and Mmul_8.0.1. With the genome of donor cell as a reference, nucleotide conversions in the edited samples that are identical to the Mmul_8.0.1 can be identified as off-target DNA SNVs as well. Note that our off-target evaluation is based on the whole embryos, and different cell types might display small differences, although with similar trends. The mechanism of ABEmax is universal across species, and ABEmax works well in plants, mice, and humans (*2*, *6*, *7*). In summary, our study demonstrates that ABEmax induces off-target RNA mutations in nonhuman primates and suggests the need to fully characterize off-target effects of ABEs.

MATERIALS AND METHODS

Animals

The rhesus monkeys (*Macaca mulatta*) facility in this study is accredited by Association for Assessment and Accreditation of Laboratory Animal Care International, and all experimental protocols were approved in advance by the Institutional Animal Care and Use Committee of the State Key Laboratory of Primate Biomedical Research with permission number LPBR202001008. The animals were housed in a controlled environment (temperature, 22° ± 1°C; humidity, 50 ± 5% relative humidity) with 12-hour light/12-hour dark cycle (lights on at 8:00 a.m.). All animals were given commercial monkey diet twice a day with tap water ad libitum and were fed fruits and vegetables daily. During and after experiments, monkeys have been under careful veterinary oversight to ensure good health. They were never involved in previous procedures and were drug and/or test naïve.

Superovulation and oocyte collection

Healthy female monkeys, ranging in ages 6 to 12 years with body weights of 5 to 8 kg, were selected for use in this study. The ovarian stimulation and oocyte recovery were performed as previously described (*13*). Briefly, healthy female monkeys with regular menstrual cycles were selected as oocyte donors for superovulation, which were performed by twice-daily intramuscular injection of 18.75 IU

of recombinant human follicle-stimulating hormone (rhFSH) (recombinant human follitropin alfa, GONAL-f, Merck Serono) for 8 days and then 1000 IU of recombinant human chorionic gonadotropin (rhCG) (recombinant human chorionic gonadotropin alfa, OVIDREL, Merck Serono) on day 9. Cumulus-oocyte complexes were collected by laparoscopic follicular aspiration 32 to 35 hours after rhCG administration. Follicular contents were placed in TALP (Hepes-buffered Tyrode's albumin lactate pyruvate) medium containing 0.3% bovine serum albumin (BSA; A8806, Sigma-Aldrich) at 37°C. Oocytes were stripped of cumulus cells by pipetting after brief exposure (<1 min) to hyaluronidase (0.5 mg/ml; H3506, Sigma-Aldrich) in TALP buffer to allow visual selection of MII (first polar body present) oocytes. The collected oocytes were cultured in the pre-equilibrated 50-μl drops of Connaught Medical Research Laboratories (DMEM) medium (11530037, Gibco) containing 10% fetal bovine serum (FBS; 04-001-1B, Biological Industries) and covered with mineral oil (M8410, Sigma-Aldrich) at 37°C with 5% CO_2.

The efficiency test of sgRNA in GFP-239T cell line

The plasmid pGL3-U6-sgRNA-PGK-puromycin (51133, Addgene) was digested with Bsa I, and then sgRNA-GFP was cloned in pGL3-U6-sgRNA-PGK-puromycin by primer annealing. Then, we changed plasmid pCMV_ABEmax_P2A_GFP (112101, Addgene) into pCMV-ABEmax-P2A-mCherry. The mCherry was amplified from pLVX-EF1α-IRES-mCherry (from Z.L.'s laboratory) and digested with Eco RI and Age I. Then, the PCR products were cloned into pCMV_ABEmax_P2A_GFP, yielding the plasmid pCMV-ABEmax-P2A-mCherry. To make the sgRNA-GFP cloned into pCMV-ABEmax-P2A-mCherry, we amplified the U6-sgRNA-GFP from the pGL3-U6-sgRNA-GFP-PGK-puromycin. Then, the PCR products and pCMV-ABEmax-P2A-mCherry were digested with Mlu I and were ligated together. The GFP-293T cells (3×10^5 cells per well in 12-well plate) were cultured with Dulbecco's modified Eagle's medium (Gibco) containing 10% FBS (Biological Industries, BI) and 1% penicillin-streptomycin (Invitrogen). Then, transfection was performed with Lipofectamine 2000 (Invitrogen) and plasmids according to the manufacturer's protocol. All cells were harvested 48 hours after transfection and isolated genomic DNA to examine the site-specific gene modification by PCR amplification. The PCR products were cloned using the pClone007 Simple Vector Kit (TSV-007S, TSINGKE) and identified by Sanger sequencing. After 7 days, the GFP was disappeared by observing in fluorescence microscope. The proportion of GFP-negative cells was analyzed by fluorescence-activated cell sorting.

Preparation of mRNA and sgRNA

pCMV_AB4Emax_P2A_GFP plasmid was linearized with the restriction enzyme Pme I, and mRNA was synthesized and purified using an in vitro RNA transcription kit (mMESSAGE mMACHINE T7 Ultra kit, AM1345, Ambion). sgRNA oligos were amplified and transcribed in vitro using the GeneArt Precision gRNA Synthesis Kit (A29377, Thermo Fisher Scientific) and purified with the MEGAclear Kit (AM1908, Thermo Fisher Scientific) according to the manufacturer's instructions.

Fibroblast cell culture and preparation of nuclear donor cells

A piece of skin tissue was obtained from the ear of the 12-year-old transgenic rhesus monkey. By washing three times in phosphate-buffered saline (PBS) containing penicillin and streptomycin, the tissue was cut into small pieces and cultured in a 6-cm culture dish. The fibroblast cells that migrated away from the tissue explants after 7 days were cultured in a 10-cm dish until they reached confluency, passaged by one-third dilution every 3 days, or disaggregated by trypsin and stored in liquid nitrogen in cell culture medium containing 10% dimethyl sulfoxide (D2650, Sigma-Aldrich). Frozen fibroblasts (passage 0 to passage 5) were thawed and cultured until confluency and used for SCNT at least 7 days later.

Monkey SCNT and ABEmax injection

MII oocytes were obtained by superovulation of female rhesus monkeys. The spindle was removed from the oocyte under spindle viewer system. After a short-term incubation with Sendai virus (HVJ Envelope/HVJ-E; ISK-CF-001-EX, GenomONE), the donor cell with GFP expression was inserted under the zona pellucida with laser lesion of zona pellucida; the fusion will be completed after 1.5 to 2 hours. The "reconstructed" oocytes were activated with ionomycin calcium salt for 5 min and treated with 6-dimethylaminopurine (D2629, Sigma-Aldrich) for 5 hours, and 10 nM TSA (trichostatin A; T8552, Sigma-Aldrich) were used to treat SCNT embryos for 10 hours during and after activation. To facilitate the epigenetic reprogramming of the somatic nucleus, the injection of H3K9me3 demethylase KDM4D mRNA (1000 ng/μl, 10 pl) were performed at 6 hours after activation, using microinjection system (Eppendorf FemtoJet 4i). For ABEmax-editing group, the RNA injection was preformed 6 to 8 hours after activation, the zygotes were injected with a mixture of ABEmax mRNA (100 ng/μl) and sgRNA (50 ng/μl) with a total volume of 1 pl for each zygote. Microinjections were performed in the cytoplasm of oocytes using a microinjection system under standard conditions.

Embryo culture and embryo transplantation

After TSA treatment, SCNT embryos were incubated in pre-equilibrated hamster embryo culture medium 9 (HECM-9) medium at 37.5°C with 5% CO_2, and the medium was changed every 48 hours until embryo transfer. The cleaved embryos with high quality at the two-cell to blastocyst stage were transferred into the oviduct of the matched recipient monkeys as described (*21*). A total of 49 rhesus female monkeys at 5 to 10 years old with proper estradiol (E2) and progesterone (P4) hormonal level were used as surrogate recipients. Three to five embryos were transferred for each recipient monkey. The earliest pregnancy diagnosis was performed by ultrasonography about 25 days after embryo transfer. Both clinical pregnancy and number of fetuses were confirmed by fetal cardiac activity and presence of yolk sac as detected by ultrasonography (*22*).

Genomic DNA extraction and sequencing

The genomic DNA from 293T, fibroblast cells, and tissues were extracted by Wizard Genomic DNA Purification Kit (A1125, Promega) according to the manufacturer's instructions. The genomic DNA of embryos was extracted by REPLI-g Single Cell Kit (150343, QIAGEN) for PCR genotyping according to manufacturer's instructions. Sanger sequencing after PCR was performed with primers as follows: forward, 5′-GACGTAAACGGCCACAAGTT-3′; reverse, 5′-GATGTTGTGGCGGATCTTGAAGTTC-3′.

Genetic analysis of cloned monkey

Genetic analysis of cloned monkey was performed as previously described (*23*). For STR analysis, ear tissue samples were collected from the monkey and used to extract DNA. Locus-specific primers

containing fluorescent dye (FAM/HEX/TMR) were used for PCR amplification. Fluorescent dye–labeled STR amplicons were diluted and mixed with internal size standard ROX500 and deionized formamide and then capillary-electrophoresed on ABI PRISM 3730 genetic analyzer to obtain the raw data. The resulted raw data were analyzed with the program GeneMarker 2.2.0, which produces Excel documents including size and genotype information, DNA profiles, and wave plots.

For SNP analysis, ear tissue samples were collected from the monkey and used to extract DNA. PCR with specific primers (forward, 5′-CCACTTCACATCAAACCATCACTT-3′; reverse, 5′-CAAGCAGCGAATACCAGCAAAA-3′) in mtDNA was performed. DNA was amplified with 35 cycles for 95°C for 30 s, 55°C for 30 s, and 72°C for 1 min, followed by a 10-min extension at 72°C. The PCR products were used for sequencing, and the results were used for the SNP analysis.

Immunostaining

For cell immunostaining, about 1×10^5 cells were seeded into 24-well plates. After adherent culturing, the cells were fixed with 4% paraformaldehyde for 15 to 20 min, then permeabilized with 0.2% Triton X-100, and blocked with 3% BSA in PBS for 2 hours at room temperature (RT). Subsequently, the cells were incubated with primary antibodies (1:100; anti–lamin A/C, sc-7293, Santa Cruz Biotechnology) overnight at 4°C and washed three times with PBS for 20 min, followed by incubating Alexa Fluor 594 (1:500; 33510, Invitrogen) for 2 hours at RT. For tissues immunofluorescent, tissues were sliced and washed with PBS. Last, the cells/tissues were stained with 4′,6-diamidino-2-phenylindole and mounted using adhesion antifade medium.

WGS and data analysis

A total of 26 samples (11 SCNT, 11 SCNT-ABE, and 4 donor cell samples) were used in the WGS analysis. These include nine SCNT and eight SCNT-ABE blastocysts, two tissues (head and body) from an aborted SCNT monkey, and three tissues (muscle, skin, and stomach) from the newborn SCNT-ABE monkey. The GFP^+ fibroblast sample (SCNT-GFP), as a SCNT donor cells, was whole-genome sequenced and used as an alternative reference genome for identifying off-target editing sites. The genomic DNA of all samples was extracted and sequenced by Illumina HiSeq X Ten. The average sequencing clean data generated for each sample were 92 Gb, with the average depth of >60×.

The workflow of whole-genome off-target SNV analysis was shown in fig. S5A. Besides SNVs, genomic copy number alterations and complex SVs were also analyzed using CNVkit (v0.9) (*24*) and DELLY (v0.8) (*25*), respectively, with default parameters. We used DELLY to detect five types of SVs: large deletion, large insertion, duplication, inversion, and translocation.

Step 1: Read mapping

The raw data were filtered and trimmed using fastp software (v0.20.0) with the base quality value of ≥25 (*26*). The qualified short reads were mapped to the reference genome of *M. mulatta* (Mmul_8.0.1 from the ensemble) using Burrows-Wheeler Aligner (BWA) (v0.7.17) MEM algorithm (*27*). After the initial alignment, SAMtools (v1.9) was used to filter multiple mapping reads (mapping quality, <30) and sort-aligned BAM files (*28*). After Q30 filtering and sorting, Sambamba (v0.7) markdup was run to remove duplicate reads in the mapped BAM files (*29*).

Step 2: SNV calling and filter

To identify the genome wide de novo variants with high confidence, we conducted SNV calling from deduplicated BAM files using four software: GATK (v4.1), LoFreq2 (v2.1.3), Strelka2 (v2.9.0), and Platypus (v0.8.1), separately (*30*–*33*). The raw SNVs were filtered using multiple filtrations: "QUAL > 30," "MQ > 30," "GQ > 30," "DP > 20" and repeat regions filtering as previous study (*34*). We only considered variants with allele frequencies more than 10% to be reliable and retained in our following analysis. Before identifying off-target SNVs, we tested whether there is interference of possible additional SNPs from the different embryo manipulation and DNA extract procedures (fig. S15). We compared the total number of SNVs called by GATK between the DNA samples from the embryos and tissues (fig. S15A), donor cells, and SCNT embryos (fig. S15B), separately. We found no difference in these samples, and this indicated that the embryo manipulation and genome extract procedure would not influence the final outcomes of the identified off-target SNVs.

Step 3: Identifying off-target SNVs

The filtered SNVs were used for identifying SCNT-ABE off-target SNVs. The background variants of the 11 SCNT and 11 SCNT-ABE samples were removed by filtering with National Center for Biotechnology Information dbSNP (Single Nucleotide Polymorphism Database) (www.ncbi.nlm.nih.gov/snp); the variant data were obtained from 81 monkeys population reported in 2018 (*35*) and other unrelated monkeys in our laboratory. After multiple filtrations and removing background variants, the reference genome (Mmul_8.0.1) was used to identify off-target SNVs. To take full advantage of SCNT, the genome of donor cell (SCNT-GFP) was used as another reference genome to identify off-target SNVs because all samples of SCNT and SCNT-ABE were derived from it. For the SNVs identified in the mapped BAM file of SCNT-ABE samples, with the SCNT samples as control, only the SNVs that mutated in the SCNT-ABE samples but not in any SCNT samples could be considered as off-target SNVs. To make the comparison, we also called the de novo variants in the SCNT sample with SCNT-ABE samples as control. Only variants mutated in the SCNT sample but not in any SCNT-ABE samples could be considered de novo variants in SCNT. In parallel, four software, GATK, Lofreq2, Strelka2, and Platypus, separately, were used to identify off-target SNVs in SCNT-ABE samples. We take the intersection of results from four software as final off-target SNVs. The genic and intergenic regions of SNVs were annotated using ANNOVAR software (version 2018-04-16) based on the RefSeq Database (*36*).

RNA-seq and data analysis

Samples from five SCNT and five SCNT-ABE blastocysts were extracted by SMART-Seq v4 Ultra Low Input RNA Kit (634896, Takara) and used for high-throughput mRNA sequencing using Illumina HiSeq. According to GATK best practices for RNA-seq variant calling, the workflow of RNA off-target SNVs analysis was shown in fig. S5B. The fastp tool (v0.20.0) was used for quality control. Qualified reads were mapped to the reference genome of *M. mulatta* (Mmul_8.0.1 from the ensemble) using STAR (2.7.1a) in two-pass mode with default parameters. Sambamba (v0.7) was then applied to sort and mark duplicates of the mapped BAM files. The refined BAM files were subject to split reads that spanned splice junctions and variant calling with SplitNCigarReads and HaplotypeCaller tools from GATK (v4.1), respectively. To identify variants with high

confidence, we filtered out the clustered variants (more than three variants within 35 bp) and retained variants with a base quality score of >25, a mapping quality score of >20, Fisher strand values of >30.0, qual by depth values of <2.0, and a sequencing depth of >20. From all called variants, downstream analyses focused solely on SNVs on canonical (one to 20, X, and Y) chromosomes. The whole-genome sequenced donor cell (SCNT-GFP) was used as reference genome. Only the SNVs that mutated in the SCNT-ABE samples but not in any SCNT samples could be considered as off-target SNVs. The editing rate was calculated as the number of mutated reads divided by the sequencing depth for each site. The adjacent 3-bp sequences of the off-target mutations were extracted from the reference genome and subjected to motif generation using R package ggseqlogo (*37*).

Quantification of gene expression, gene ontology enrichment, and related gene set

Gene expression was inferred from the refined BAM files using featureCounts (v1.6.4) (*38*) and reported as transcripts per million. Gene ontology (GO) biological processes enrichment was performed using the functions "enrichr" in clusterProfiler R package (*39*). The cancer-related genes were retrieved from the Cancer Gene Census (https://cancer.sanger.ac.uk). The key genes for early embryonic development of rhesus monkey were obtained from the study of Liu's laboratory (*23*).

SUPPLEMENTARY MATERIALS

Supplementary material for this article is available at https://science.org/doi/10.1126/sciadv.abo3123

View/request a protocol for this paper from *Bio-protocol*.

REFERENCES AND NOTES

1. A. C. Komor, Y. B. Kim, M. S. Packer, J. A. Zuris, D. R. Liu, Programmable editing of a target base in genomic DNA without double-stranded DNA cleavage. *Nature* **533**, 420–424 (2016).
2. N. M. Gaudelli, A. C. Komor, H. A. Rees, M. S. Packer, A. H. Badran, D. I. Bryson, D. R. Liu, Programmable base editing of A*T to G*C in genomic DNA without DNA cleavage. *Nature* **551**, 464–471 (2017).
3. T. Rothgangl, M. K. Dennis, P. J. C. Lin, R. Oka, D. Witzigmann, L. Villiger, W. Qi, M. Hruzova, L. Kissling, D. Lenggenhager, C. Borrelli, S. Egli, N. Frey, N. Bakker, J. A. Walker, A. P. Kadina, D. V. Victorov, M. Pacesa, S. Kreutzer, Z. Kontarakis, A. Moor, M. Jinek, D. Weissman, M. Stoffel, R. van Boxtel, K. Holden, N. Pardi, B. Thöny, J. Häberle, Y. K. Tam, S. C. Semple, G. Schwank, In vivo adenine base editing of *PCSK9* in macaques reduces LDL cholesterol levels. *Nat. Biotechnol.* **39**, 949–957 (2021).
4. K. Musunuru, A. C. Chadwick, T. Mizoguchi, S. P. Garcia, J. E. DeNizio, C. W. Reiss, K. Wang, S. Iyer, C. Dutta, V. Clendaniel, M. Amaonye, A. Beach, K. Berth, S. Biswas, M. C. Braun, H.-M. Chen, T. V. Colace, J. D. Ganey, S. A. Gangopadhyay, R. Garrity, L. N. Kasiewicz, J. Lavoie, J. A. Madsen, Y. Matsumoto, A. M. Mazzola, Y. S. Nasrullah, J. Nneji, H. Ren, A. Sanjeev, M. Shay, M. R. Stahley, S. H. Y. Fan, Y. K. Tam, N. M. Gaudelli, G. Ciaramella, L. E. Stolz, P. Malyala, C. J. Cheng, K. G. Rajeev, E. Rohde, A. M. Bellinger, S. Kathiresan, In vivo CRISPR base editing of *PCSK9* durably lowers cholesterol in primates. *Nature* **593**, 429–434 (2021).
5. L. W. Koblan, M. R. Erdos, C. Wilson, W. A. Cabral, J. M. Levy, Z. M. Xiong, U. L. Tavarez, L. M. Davison, Y. G. Gete, X. Mao, G. A. Newby, S. P. Doherty, N. Narisu, Q. Sheng, C. Krilow, C. Y. Lin, L. B. Gordon, K. Cao, F. S. Collins, J. D. Brown, D. R. Liu, In vivo base editing rescues Hutchinson-Gilford progeria syndrome in mice. *Nature* **589**, 608–614 (2021).
6. E. Zuo, Y. Sun, W. Wei, T. Yuan, W. Ying, H. Sun, L. Yuan, L. M. Steinmetz, Y. Li, H. Yang, Cytosine base editor generates substantial off-target single-nucleotide variants in mouse embryos. *Science* **364**, 289–292 (2019).
7. S. Jin, Y. Zong, Q. Gao, Z. Zhu, Y. Wang, P. Qin, C. Liang, D. Wang, J.-L. Qiu, F. Zhang, C. Gao, Cytosine, but not adenine, base editors induce genome-wide off-target mutations in rice. *Science* **364**, 292–295 (2019).
8. C. Zhou, Y. Sun, R. Yan, Y. Liu, E. Zuo, C. Gu, L. Han, Y. Wei, X. Hu, R. Zeng, Y. Li, H. Zhou, F. Guo, H. Yang, Off-target RNA mutation induced by DNA base editing and its elimination by mutagenesis. *Nature* **571**, 275–278 (2019).
9. J. Grunewald, R. Zhou, S. P. Garcia, S. Iyer, C. A. Lareau, M. J. Aryee, J. K. Joung, Transcriptome-wide off-target RNA editing induced by CRISPR-guided DNA base editors. *Nature* **569**, 433–437 (2019).
10. H. A. Rees, C. Wilson, J. L. Doman, D. R. Liu, Analysis and minimization of cellular RNA editing by DNA adenine base editors. *Sci. Adv.* **5**, eaax5717 (2019).
11. H. S. Kim, Y. K. Jeong, J. K. Hur, J.-S. Kim, S. Bae, Adenine base editors catalyze cytosine conversions in human cells. *Nat. Biotechnol.* **37**, 1145–1148 (2019).
12. L. W. Koblan, J. L. Doman, C. Wilson, J. M. Levy, T. Tay, G. A. Newby, J. P. Maianti, A. Raguram, D. R. Liu, Improving cytidine and adenine base editors by expression optimization and ancestral reconstruction. *Nat. Biotechnol.* **36**, 843–846 (2018).
13. Y. Niu, Y. Yu, A. Bernat, S. Yang, X. He, X. Guo, D. Chen, Y. Chen, S. Ji, W. Si, Y. Lv, T. Tan, Q. Wei, H. Wang, L. Shi, J. Guan, X. Zhu, M. Afanassieff, P. Savatier, K. Zhang, Q. Zhou, W. Ji, Transgenic rhesus monkeys produced by gene transfer into early-cleavage–stage embryos using a simian immunodeficiency virus-based vector. *Proc. Natl. Acad. Sci. U.S.A.* **107**, 17663–17667 (2010).
14. X. Zhang, S. Gao, X. Liu, Advance in the role of epigenetic reprogramming in somatic cell nuclear transfer-mediated embryonic development. *Stem Cells Int.* **2021**, 16681337 (2021).
15. X. Yang, S. L. Smith, X. C. Tian, H. A. Lewin, J. P. Renard, T. Wakayama, Nuclear reprogramming of cloned embryos and its implications for therapeutic cloning. *Nat. Genet.* **39**, 295–302 (2007).
16. Z. Ao, D. Liu, C. Zhao, Z. Yue, J. Shi, R. Zhou, G. Cai, E. Zheng, Z. Li, Z. Wu, Birth weight, umbilical and placental traits in relation to neonatal loss in cloned pigs. *Placenta* **57**, 94–101 (2017).
17. C. R. Lazzarotto, N. T. Nguyen, X. Tang, J. Malagon-Lopez, J. A. Guo, M. J. Aryee, J. K. Joung, S. Q. Tsai, Defining CRISPR-Cas9 genome-wide nuclease activities with CIRCLE-seq. *Nat. Protoc.* **13**, 2615–2642 (2018).
18. K. R. Anderson, M. Haeussler, C. Watanabe, V. Janakiraman, J. Lund, Z. Modrusan, J. Stinson, Q. Bei, A. Buechler, C. Yu, S. R. Thamminana, L. Tam, M. A. Sowick, T. Alcantar, N. O'Neil, J. Li, L. Ta, L. Lima, M. Roose-Girma, X. Rairdan, S. Durinck, S. Warming, CRISPR off-target analysis in genetically engineered rats and mice. *Nat. Methods* **15**, 512–514 (2018).
19. D. Kim, K. Lim, S. T. Kim, S. H. Yoon, K. Kim, S. M. Ryu, J. S. Kim, Genome-wide target specificities of CRISPR RNA-guided programmable deaminases. *Nat. Biotechnol.* **35**, 475–480 (2017).
20. S. Q. Tsai, J. K. Joung, Defining and improving the genome-wide specificities of CRISPR-Cas9 nucleases. *Nat. Rev. Genet.* **17**, 300–312 (2016).
21. H. Liu, Y. Chen, Y. Niu, K. Zhang, Y. Kang, W. Ge, X. Liu, E. Zhao, C. Wang, S. Lin, B. Jing, C. Si, Q. Lin, X. Chen, H. Lin, X. Pu, Y. Wang, B. Qin, F. Wang, H. Wang, W. Si, J. Zhou, T. Tan, T. Li, S. Ji, Z. Xue, Y. Luo, L. Cheng, Q. Zhou, S. Li, Y. E. Sun, W. Ji, TALEN-mediated gene mutagenesis in rhesus and cynomolgus monkeys. *Cell Stem Cell* **14**, 323–328 (2014).
22. Y. Chen, Y. Niu, S. Yang, H. E. Xiechao, J. I. Shaohui, S. I. Wei, X. Tang, Y. Xie, H. Wang, Y. Lu, Q. Zhou, W. Ji, The available time window for embryo transfer in the rhesus monkey (*Macaca mulatta*). 74, 165–173 (2012).
23. Z. Liu, Y. Cai, Y. Wang, Y. Nie, C. Zhang, Y. Xu, X. Zhang, Y. Lu, Z. Wang, M. Poo, Q. Sun, Cloning of macaque monkeys by somatic cell nuclear transfer. *Cell* **172**, 881–887.E7 (2018).
24. E. Talevich, A. H. Shain, T. Botton, B. C. Bastian, CNVkit: Genome-wide copy number detection and visualization from targeted DNA sequencing. *PLoS Comput. Biol.* **12**, e1004873 (2016).
25. T. Rausch, T. Zichner, A. Schlattl, A. M. Stutz, V. Benes, J. O. Korbel, DELLY: Structural variant discovery by integrated paired-end and split-read analysis. *Bioinformatics* **28**, i333–i339 (2012).
26. S. Chen, Y. Zhou, Y. Chen, J. Gu, fastp: An ultra-fast all-in-one FASTQ preprocessor. *Bioinformatics* **34**, i884–i890 (2018).
27. H. Li, R. Durbin, Fast and accurate short read alignment with Burrows-Wheeler transform. *Bioinformatics* **25**, 1754–1760 (2009).
28. H. Li, B. Handsaker, A. Wysoker, T. Fennell, J. Ruan, N. Homer, G. Marth, G. Abecasis, R. Durbin; 1000 Genome Project Data Processing Subgroup, The Sequence Alignment/Map format and SAMtools. *Bioinformatics* **25**, 2078–2079 (2009).
29. A. Tarasov, A. J. Vilella, E. Cuppen, I. J. Nijman, P. Prins, Sambamba: Fast processing of NGS alignment formats. *Bioinformatics* **31**, 2032–2034 (2015).
30. S. Kim, K. Scheffler, A. L. Halpern, M. A. Bekritsky, E. Noh, M. Kallberg, X. Chen, Y. Kim, D. Beyter, P. Krusche, C. T. Saunders, Strelka2: Fast and accurate calling of germline and somatic variants. *Nat. Methods* **15**, 591–594 (2018).
31. A. McKenna, M. Hanna, E. Banks, A. Sivachenko, K. Cibulskis, A. Kernytsky, K. Garimella, D. Altshuler, S. Gabriel, M. Daly, M. A. DePristo, The Genome Analysis Toolkit: A MapReduce framework for analyzing next-generation DNA sequencing data. *Genome Res.* **20**, 1297–1303 (2010).
32. A. Rimmer, H. Phan, I. Mathieson, Z. Iqbal, S. R. F. Twigg, W. G. S. Consortium, A. O. M. Wilkie, G. McVean, G. Lunter, Integrating mapping-, assembly- and haplotype-based approaches for calling variants in clinical sequencing applications. *Nat. Genet.* **46**, 912–918 (2014).

33. A. Wilm, P. P. Aw, D. Bertrand, G. H. Yeo, S. H. Ong, C. H. Wong, C. C. Khor, R. Petric, M. L. Hibberd, N. Nagarajan, LoFreq: A sequence-quality aware, ultra-sensitive variant caller for uncovering cell-population heterogeneity from high-throughput sequencing datasets. *Nucleic Acids Res.* **40**, 11189–11201 (2012).
34. X. Luo, Y. He, C. Zhang, X. He, L. Yan, M. Li, T. Hu, Y. Hu, J. Jiang, X. Meng, W. Ji, X. Zhao, P. Zheng, S. Xu, B. Su, Trio deep-sequencing does not reveal unexpected off-target and on-target mutations in Cas9-edited rhesus monkeys. *Nat. Commun.* **10**, 5525 (2019).
35. Z. Liu, X. Tan, P. Orozco-terWengel, X. Zhou, L. Zhang, S. Tian, Z. Yan, H. Xu, B. Ren, P. Zhang, Z. Xiang, B. Sun, C. Roos, M. W. Bruford, M. Li, Population genomics of wild Chinese rhesus macaques reveals a dynamic demographic history and local adaptation, with implications for biomedical research. *Gigascience* **7**, giy106 (2018).
36. K. Wang, M. Li, H. Hakonarson, ANNOVAR: Functional annotation of genetic variants from high-throughput sequencing data. *Nucleic Acids Res.* **38**, e164 (2010).
37. O. Wagih, ggseqlogo: A versatile R package for drawing sequence logos. *Bioinformatics* **33**, 3645–3647 (2017).
38. Y. Liao, G. K. Smyth, W. Shi, featureCounts: An efficient general purpose program for assigning sequence reads to genomic features. *Bioinformatics* **30**, 923–930 (2014).
39. G. Yu, L.-G. Wang, Y. Han, Q.-Y. He, clusterProfiler: An R package for comparing biological themes among gene clusters. *OMICS* **16**, 284–287 (2012).

Acknowledgments: We thank T. Li and Y. Yin for provide pLVX-EF1α-IRES-mCherry plasmid in this study. We also thank Z. Zhao, Y. Zhou, H. Ma, and W. Han for help in animal care.

Funding: This work was supported by the National Key Research and Development Program of China (2018YFA0801403, 2021YFA1102003, and 2021YFA0805702), the National Natural Science Foundation of China (U2102204), and the Natural Science Foundation of Yunnan Province (202001BC070001 and 202102AA100053). **Author contributions:** Conceptualization: Y.N. and W.J. Methodology: Y.N., Y.K., S.D., Y.Z., Z.Y., and W.S. Investigation: Y.K., S.D., Y.Z., and F.W. Visualization: S.D., P.Y., and Y.P. Animal care: Z.L., B.T., and X.C. Project administration: Y.N. Supervision: Y.N. and W.J. Writing (original draft): Y.K., S.D., Y.Z., and Y.N. Writing (review and editing): All authors. **Competing interests:** The authors declare that they have no competing interests. **Data and materials availability:** The raw sequence data reported in this paper have been deposited in the Genome Sequence Archive in the National Genomics Data Center, Chinese Academy of Sciences, under accession number CRA004092 that are publicly accessible at https://ngdc.cncb.ac.cn/gsa. All the Python and R codes for DNA and RNA off-target SNV analysis in the study are deposited in Zenodo under accession number 6605030 (https://doi.org/10.5281/zenodo.6605030). These codes are also available at https://github.com/daishaoxing/OA-SCNT. The plasmids used in base editing can be provided by Addgene pending scientific review and a completed material transfer agreement. Requests for the plasmids should be submitted to Addgene. All data needed to evaluate the conclusions in the paper are present in the paper and/or the Supplementary Materials.

Submitted 27 January 2022
Accepted 9 June 2022
Published 22 July 2022
10.1126/sciadv.abo3123